2016

Analysis of the Measurements Reliability in Dynamic Test of the Opaque Envelope

Nadja Bishara
Free University of Bozen, Italy, nadja.bisharaschroetter@natec.unibz.it

Alessandro Prada
Free University of Bozen, Italy, alessandro.prada@unibz.it

Giovanni Pernigotto
Free University of Bozen, Italy, giovanni.pernigotto@unibz.it

Marco Baratieri
Free University of Bozen, Italy, marco.baratieri@unibz.it

Andrea Gasparella
Free University of Bozen, Italy, andrea.gasparella@unibz.it

Analysis of the measurements reliability in dynamic test of the opaque envelope

Nadja BISHARA[1]*, Alessandro PRADA[2], Giovanni PERNIGOTTO[3], Marco BARATIERI[4] and Andrea GASPARELLA[5]

[1]Free University of Bozen-Bolzano, Faculty of Science and Technology, Bolzano, Italy
Tel: +39 0471 017685, Fax: +39 0471 017009, nadja.bisharaschroetter@natec.unibz.it

[2]University of Trento, Department of Civil Environmental and Mechanical Engineering, Trento, Italy
Tel: +39 0461 282653, Fax: +39 0461 282672, email: alessandro.prada@unitn.it

[3]Free University of Bozen-Bolzano, Faculty of Science and Technology, Bolzano, Italy
Tel: +39 0471 017632, Fax: +39 0471 017009, email: giovanni.pernigotto@unibz.it

[4]Free University of Bozen-Bolzano, Faculty of Science and Technology, Bolzano, Italy
Tel: +39 0471 017201, Fax: +39 0471 017009, email: marco.baratieri@unibz.it

[5]Free University of Bozen-Bolzano, Faculty of Science and Technology, Bolzano, Italy
Tel: +39 0471 017200, Fax: +39 0471 017009, email: andrea.gasparella@unibz.it

*Corresponding Author

ABSTRACT

The characterization of opaque building components' thermal behavior is essential in early design stages to compare different design and refurbishment alternatives. Evaluating the dynamic thermal response to an external solicitation is necessary for an effective design especially for the climates with important annual cooling demand. According to EN ISO 13786:2007, opaque elements can be characterized through some dynamic parameters (i.e., periodic thermal transmittance, decrement factor and time shift), which can be calculated starting from the wall materials' thermal properties. However, when either the material thermo-physical properties are unknown (e.g., in existing buildings) or the assumptions about 1-dimensional heat flux on which the method is based are not met (e.g., in platform-frame structures), proper accuracy of results is not ensured. Hence, for these cases and components, a direct measurement of dynamic parameters would be extremely useful.
Differently from the procedure to determine the steady-state thermal transmission properties, which is well established, there are no technical standards defined for the experimental measurement of dynamic thermal parameters so far. Since these experimental procedures are still under development, the extent to which several aspects limit accuracy and precision of the measurements are not yet cleared. In this framework, this paper presents both experimental and numerical tests, which have been performed in order to assess the impact of different sources of uncertainty on the estimation of EN ISO 13786 dynamic parameters by means of heat flux meter measurements on a timber wall specimen.

1. INTRODUCTION

The overall energy consumption of buildings is mainly due to annual heating and cooling demand, whose relative incidence can be different according to climate and use conditions. In south Europe cities, the cooling demand can be as much important as the heating one and, for the Mediterranean localities, it can be the main cause of building energy consumption. In the current European framework (e.g., Directive 31/2010/EU) and in the EU Member legislations (e.g., Italian Minister Decree 26/06/2015), energy efficiency for space cooling has to be pursued in the first place by means of both window shading systems and adequate opaque components design. As regards the latter, an efficient opaque component has to be able to store the heat absorbed from solar irradiation and to reduce and delay its impact on the indoor energy balance. For this reason, the law provides prescriptions about the thermal parameters characterizing the dynamic performance of the opaque envelope,

relating the temperature excitations at the component's exterior surface to the heat flux responses at the interior one. According to EN ISO 13786:2007 (CEN, 2007a), these quantities are the periodic thermal transmittance, the time shift and the decrement factor. While periodic thermal transmittance and decrement factor express the ability of the component to damp the effects of unsteady solicitations, the time shift indicates the ability of delaying their impact on the internal surface heat balance. If a component's material properties are well known, the calculation of the dynamic thermal parameters can be easily performed according to the methods described by EN ISO 13786 itself. However, if the thermal material properties are not comprehensively known, as it is often in case for the existing building stock (Martín *et al.*, 2010), or in case of inhomogeneous components characterized by multi-dimensional heat flows (e.g., in platform-frame structures; Martín *et al.*, 2012), inaccurate results can be found. In those contexts, a direct measurement of dynamic thermal parameters can be necessary to overcome uncertainty, insufficient knowledge of the inputs or other issues related to the applicability of EN ISO 13786 method.

While measurement strategies for laboratory and in-situ determination of steady-state thermal properties are well-defined in technical standards, such as EN 1934:1998 (CEN, 1998), standardized procedures for an experimental determination of dynamic characteristics are still missing. Nevertheless, as it can be seen in the literature (e.g., Brown and Stephenson, 1993a and 1993b; Martín *et al.*, 2010; Martín *et al.*, 2012; Sala *et al.*, 2008; Ulgen 2002), the topic has been addressed by some researchers in the last decades, often with different points of view and targets, studying the possibility of exploiting and adapting hotbox apparatus to the measurements of EN ISO 13786 dynamic parameters. Brown and Stephenson (1993a and 1993b) experimentally investigated seven wall structures in order to evaluate their dynamic heat transmission characteristics. Other researchers compared measured and calculated dynamic parameters and found some discrepancies. Ulgen (2002) tested ten different walls and saw high differences, especially for the decrement factors. Sala *et al.* (2008) measured the dynamic thermal characteristics of differently insulated brick walls and observed significant deviations between measured and simulated response time. Martín *et al.* (2010) determined the response factors of a wall with unknown material properties, measuring the heat flux on both sides of a specimen with heat flux meters. Moreover, the authors simulated their experimental setup by means of a Computational Fluid Dynamics code, finding a good agreement between measured and simulated heat flows. A further research (Martín *et al.*, 2012) focused on the dynamic thermal response of structures including thermal bridges, revealing a difference between measured and numerically simulated amplitude of the heat flux.

According to what observed in the literature, methodologies based on hotboxes and hotboxes equipped with heat flow meters can be used for the assessment of dynamic thermal characteristics of opaque envelope components. However, the extent to which the results are affected by different sources of uncertainty is not fully clear and this makes difficult the development of in-situ dynamic measurement procedures based on heat flow meters. In this work, experimental and numerical simulations were combined in order to better understand the impact of uncertainty on the measurement of dynamic parameters. A modified hotbox and heat flow meter setup was used to test a timber wall construction under dynamic boundary conditions and a numerical model was developed and calibrated against the collected experimental data. With this model, factors affecting the measurement accuracy were analyzed and discussed.

2. METHOD

2.1 Experimental setup and procedure

Experimental investigations were performed with a modified hotbox apparatus at the building physics lab of the Free University of Bozen-Bolzano. A standard hotbox apparatus according to EN 1934:1998 consists of two climatic chambers separated by a test specimen, providing two different constant thermal conditions which generate a heat flow monitored by means of a heat flow meter (*HFM*) installed in one of the two chambers. This setup was modified by removing one chamber and installing a copper coil electrical heater very close to the test specimen's surface (Figure 1). The chamber has side lengths of 1.5 m and is equipped with PID-controlled cooling (i.e., an evaporator) and heating units (i.e., an electrical resistance). A radiant screen made of plywood is positioned within the climatic chamber, in front of the test specimen, in order to prevent radiant heat exchange with the chamber walls. A fan working constantly induces an air flow through the 3.9 cm broad gap between the screen and the wall specimen at 1.5 m s^{-1}. The electrical heater covers a wall surface area of 1.2 m by 1.2 m and generates a nominal power of 1500 W, operated cyclically for 2 h followed by a break of 22 h, in order to impose a periodic forcing solicitation of a side of the tested wall.

In this research work, we used as sample a timber wall (length 1.31 m, height 1.23 m, thickness 0.24 m) made of four parallel spruce wood layers and surrounded by insulating materials (i.e., 0.28 m of EPS plus 0.09 m of sheep wool) to minimize the lateral heat flow exchanged with the air of the lab. For the same reason, the chamber kept a constant internal temperature of 23 °C, equal to lab setpoint.

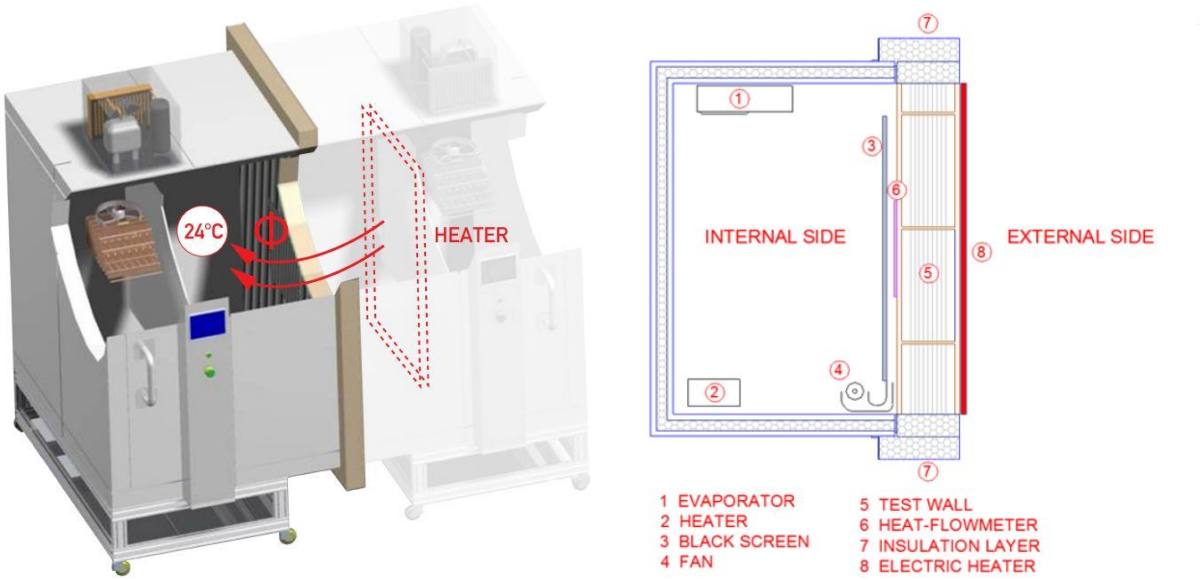

Figure 1: Experimental setup.

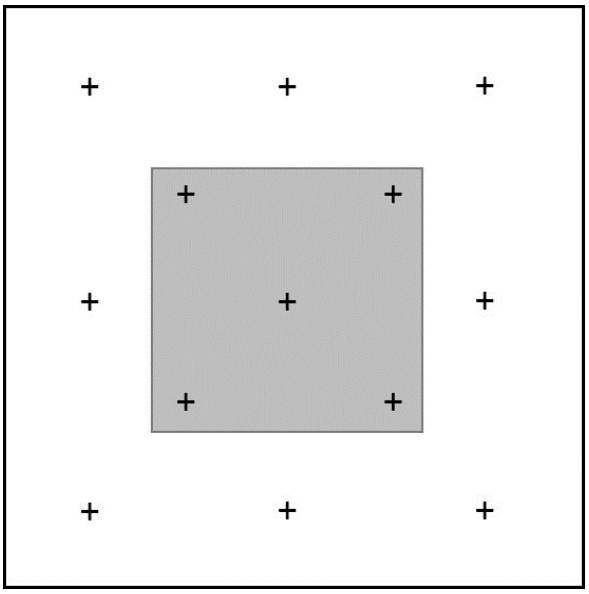

Figure 2: Schematic of the measurement setup (cross: thermocouples, grey area: *HFM*).

A set of 26 type T thermocouples measures surface temperatures at both sides of the timber wall in various positions, with one-minute time interval (Figure 2). The *HFM* used in this test, a square plate of 0.5 m by 0.5 m with an overall thickness of 0.012 m, was installed centrally with respect to the specimen's surface and consisted of a thermopile with 250 type T thermocouples. Further type T thermocouples measured the air temperature within the climatic chamber and within the laboratory environment, respectively.

2.2 Experimental evaluation of dynamic parameters

The external surface temperature and the internal surface heat flux are recorded for four days after the first three days of test. Then, the Fast Fourier Transform (*FFT*) algorithm (Press *et al.*, 2007) was applied to calculate the first 720 harmonics of external surface temperature and internal surface heat flux. For each of these days, the first term of the Fourier approximation (i.e. the fundamental one with a period of 24 h) was used to compute periodic thermal transmittance, decrement factor and time shift in accordance with EN ISO 13786:2007. Since direct measurements of surface heat flux and temperature values were collected, surface thermal resistances were neglected in these calculations. For each daily cycle, the periodic thermal transmittance Y_{ie} was computed as the ratio between the amplitude of the first harmonic of internal surface heat flux $\phi_{i,1}$ and the amplitude of the first harmonic of external surface temperature $\theta_{e,1}$:

$$Y_{i_e} = \frac{\Phi_{i,1}}{\theta_{e,1}} \tag{1}$$

The decrement factor *f* was computed by relating the periodic thermal transmittance to the steady state thermal conductance, which was found equal to 0.468 W m^{-2} K^{-1} during a preliminary steady state test:

$$f = \frac{Y_{i_e}}{C_s} \tag{2}$$

The time shift Δt_{ie} was computed using the phase displacements of the fundamental, respectively ϕ for the external temperature solicitation and ψ for the internal heat flux:

$$\theta_e \approx \overline{\theta}_e + \theta_{e,1} \cos(\omega t + \varphi) \tag{3}$$

$$\Phi_i \approx \overline{\Phi}_i + \Phi_{i,1} \cos(\omega t + \psi) \tag{4}$$

$$\Delta t_{i_e} = \frac{(\psi - \varphi)}{(2\pi)} \cdot 24 \tag{5}$$

2.3 Numerical Simulation Model

Additionally to the defined experimental model, numerical simulations were carried out with the software Delphin (Grunewald, 1997; Nicolai, 2008). Delphin 5 is a validated software (Nicolai, 2011) based on a finite control volume method, which facilitates the modelling of one- and two-dimensional heat and mass transfer processes. Aiming at an assessment of the measurement procedure and sensors reliability under dynamic conditions and at an investigation of the impact of the difference sources of uncertainty (e.g., lateral heat loss, installation of a guard ring, contact resistances), a two-dimensional numerical model was developed and calibrated against experimental data.

The model includes the timber wall specimen and an internally installed *HFM* (Figure 3). Assuming homogeneous air flow conditions on *HFM* and wall specimen, and exploiting symmetry, it was sufficient to consider a construction with half of its height merely. An equidistant grid with elements sized 1 mm by 1 mm was chosen as basic configuration, with the possibility of using elements larger up to 10 mm of height to facilitate balancing numerical errors and reducing simulation time. After some tests on some alternatives, a final simulation model with 13 952 cells was found in compliance with the criteria adopted for ensuring a normalized accuracy of residuals of 10^{-5}.

The measured surface temperatures were set as surface boundary conditions to the numerical model at the external side of the specimen, where the electrical heater was located (red dashed line in Figure 3). Top and bottom sides were defined as adiabatic, since they were well insulated and thus the heat flow through those surfaces could be assumed as negligible. Furthermore, this allowed robust findings from the adoption of 2-dimensional instead of 3-dimensional modelling as well. Differently from previous analyses (Pernigotto *et al.*, 2015), in this research the focus was put on uncertainty issues about heat transfer by conduction through the specimen and the *HFM*. Consequently, the model was limited to the solid domain and heat transfer by convection was dealt as a boundary condition to apply. Taking into consideration a model calibration, convective heat transfer coefficients were initially set according to the technical standard EN ISO 6946:2007 (CEN, 2007b): for the top of the external side of the specimen, a convective heat transfer coefficient of 7.7 W m^{-2} K^{-1} and a bulk temperature equal to the measured laboratory room temperature were set (blue line in Figure 3) while at the internal side, where forced convection was prevalent, we used a convective heat transfer coefficient of 10 W m^{-2} K^{-1}, calculated according to EN ISO 6946:2007, and the measured average air gap temperature.

Since the actual material properties of the spruce timber wall were unknown, a dry bulk density of 370 kg m^{-3}, a specific heat capacity (dry material) of 1350 J kg^{-1} K^{-1} and a thermal conductivity for a radial wood fiber direction of 0.098 W m^{-1} K^{-1} were assumed according to Kollmann (1982). Figure 4 captures an overview about the defined *HFM* geometric and thermal properties: the main layer, composed by rubber material embedding the thermopile, is positioned between an interface material and an aluminum layer, both with high thermal conductivity. *HFM* material properties were taken from manufacturer datasheets and, as regards the rubber layer, checked experimentally by means of Laser Flash Analysis.

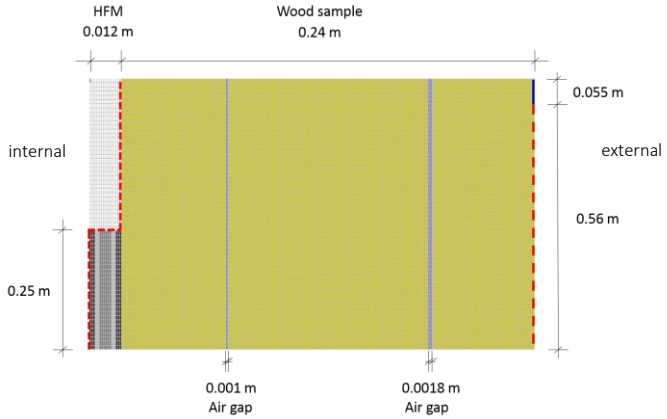

Figure 3: Structure of the numerical model.

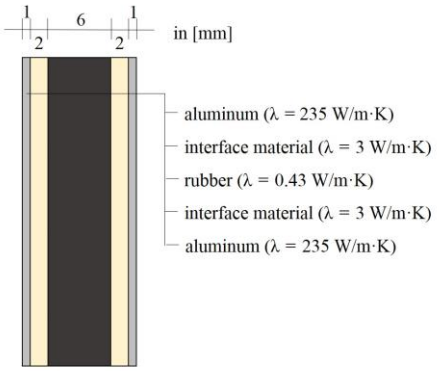

Figure 4: *HFM* geometric and thermal properties.

3. RESULTS AND DISCUSSION

3.1 Experimental results

Measured external surface temperature is shown in Figure 5 with a blue curve, reaching peak values of 52.5 °C, and minimum values of 23 °C. Filtered internal air-gap temperature, shown as red curve, averages to 23.6 °C, whereas it shows a periodically recurring unsteady behavior caused by the climatic chamber's air conditioning unit. Figure 6 shows the measured heat flux curves, both original and filtered according to second order Butterworth low-pass filter. Values move periodically in the interval between -0.5 W m^{-2} and 2.9 W m^{-2}, whereby the results show an increasing trend within the first days, due to thermal inertia effects of the test specimen.

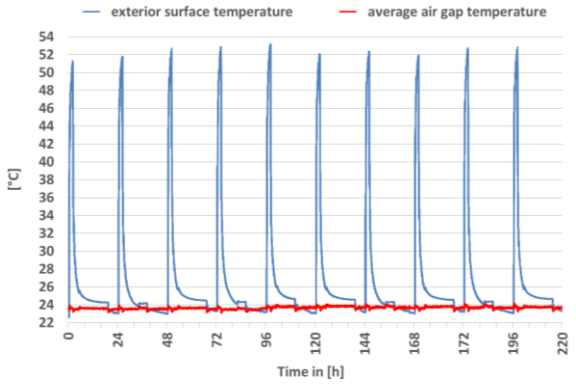

Figure 5: Measured temperature values.

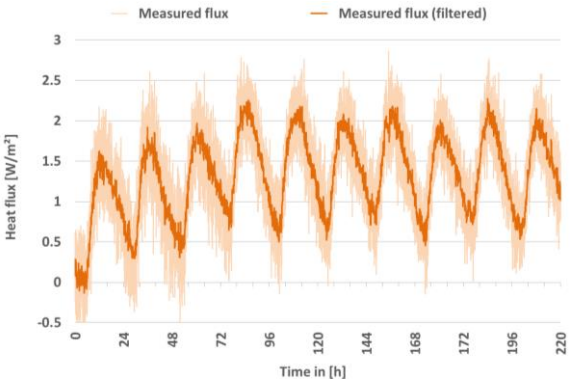

Figure 6: Measured heat flux values.

From the measured data, EN ISO 13786 dynamic parameters were calculated for each day of monitoring. Periodic thermal transmittance values averaged to 0.1285 W m^{-2} K^{-1}, decrement factor to 0.2745, and time shift to 11.67 h (Table 1).

Table 1: Dynamic thermal parameters computed from experimental measurements.

	Y_{ie} [W m^{-2} K^{-1}]	f [-]	Δt_{ie} [h]
Day 4	0.1263	0.2698	11.27
Day 5	0.1386	0.2962	11.83
Day 6	0.1301	0.2780	12.17
Day 7	0.1188	0.2540	11.42
Average	**0.1285**	**0.2745**	**11.67**

3.2 Numerical simulation results

Simulated heat flux values of a first numerical model (blue line in Figure 7) were compared to the measured results (orange curve in Figure 7): while phases match well, some disagreement can be seen between amplitudes. Furthermore, the simulated curve displays noticeable cyclic peaks, which are not so clearly observed in experimental data. As it can be seen in Figure 5 (red line), the laboratory room temperature conditions were not constant and this affected both measured and simulated heat fluxes. However, since the measured heat flux is very noisy (light orange curve in Figure 7), after the filtering process the impact of unsteady environment conditions can be hardly detected.

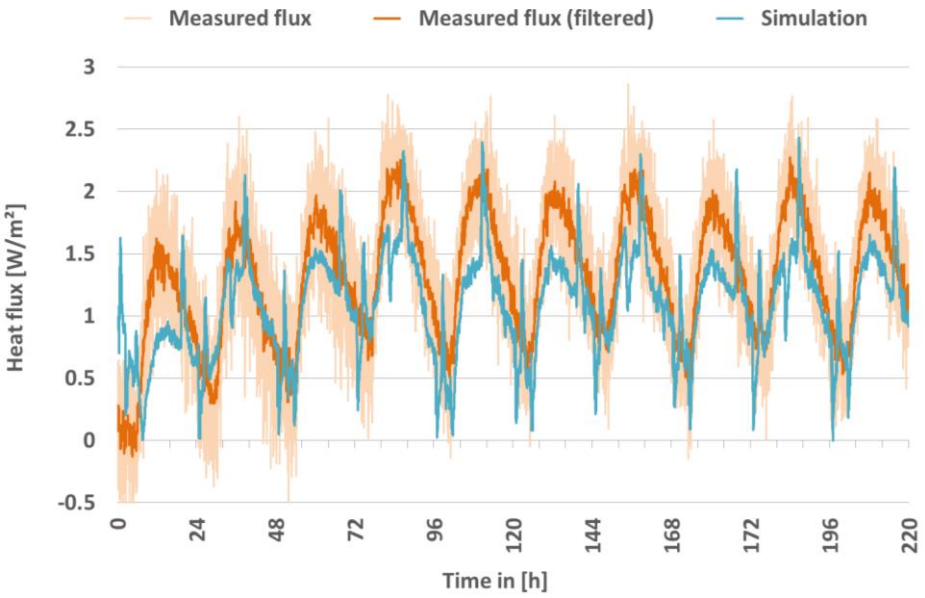

Figure 7: Measured and simulated heat flux.

3.3 Calibration of the numerical model

The preliminary numerical model achieved a good agreement only with measured phases and so a calibration process was performed against measured heat fluxes. After some preliminary sensitivity analyses, which highlighted the different impact of material properties and surface heat transfer coefficients, the calibration procedure was split into two stages.

In the first step, density and thermal conductivity of the timber wall material were adjusted, resulting in a better fit of amplitudes. Results are shown in Figure 8, for the whole measurement cycle (Figure 8a), and more in detail for the fifth and sixth day (Figure 8b). Adjusted density and thermal conductivity of spruce wood are 520 kg m^{-3}, and 0.141 W m^{-1} K^{-1}, respectively.

The second calibration phase was on the convective heat transfer coefficient at the internal surface, initially determined according to an approximated correlation. An increased constant value of 14 W m^{-2} K^{-1} led to well corresponding measured and calculated heat flux values, as it can be seen in Figure 9a and 9b.

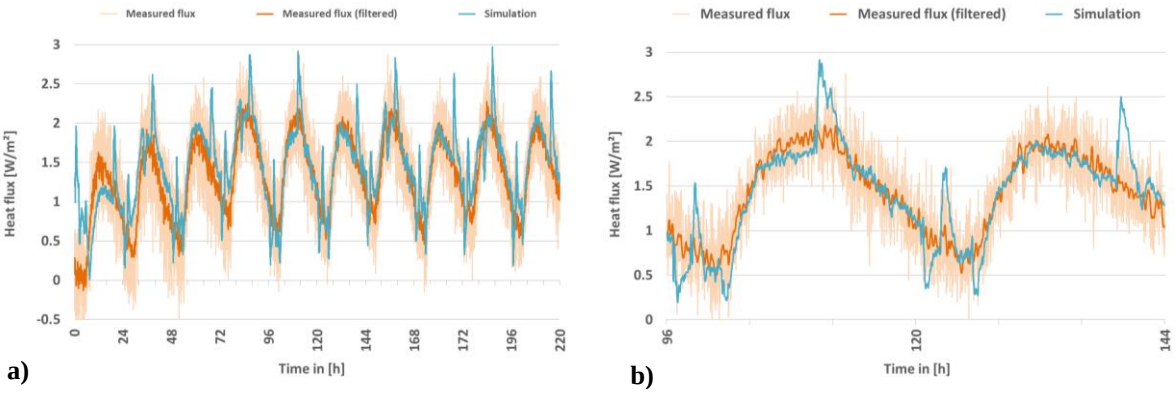

Figure 8: Results of a first calibrated numerical model - adjusted spruce wood properties.

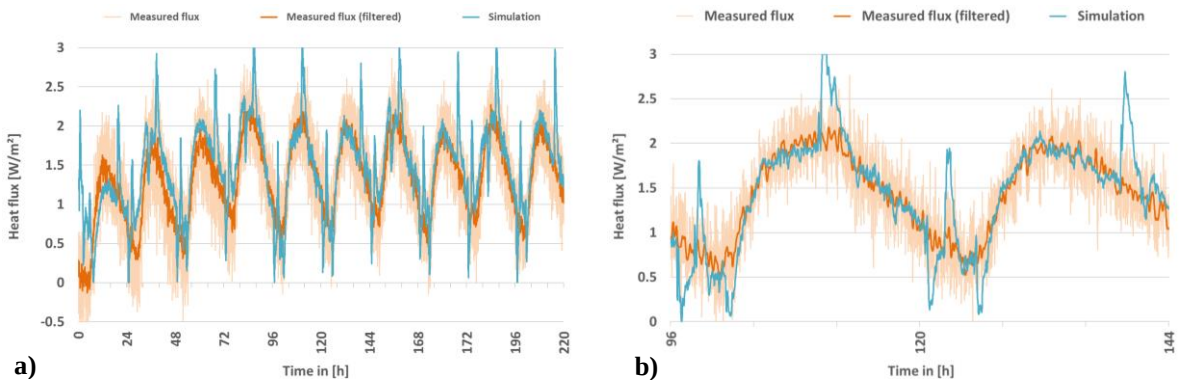

Figure 9: Results of a second calibrated numerical model - adjusted convective heat transfer coefficient.

For all models, dynamic thermal parameters were computed, basing on the first harmonics from the *FFT* analysis (Table 2). While results from a first numerical model led to high deviations from the measured average periodic thermal transmittance (-21.82 %), the calibrated numerical model presented a reduced error of 9.32 %. Moreover, deviation of the numerically achieved time shift from the measured one was very low (0.59 %).

Table 2: Dynamic thermal parameters from numerical models compared to experimental data.

	Y_{ie} [W m^{-2} K^{-1}]	Deviations from measured values	t_{ie} [h]	Deviations from measured values
Measured values	0.1285	-	11.67	-
Preliminary numerical model	0.1004	-21.82 %	11.93	2.16 %
Calibrated numerical model	0.1404	9.32 %	11.74	0.59 %

3.4 Analysis of boundary conditions

The calibrated numerical model was used to analyze the impact of different boundary conditions on the results. First, the incidence of convective conditions at the internal surface of the wall specimen was discussed. Then, we investigated the impact of some alternative experimental configurations on one-dimensional heat flux attainment (size of the *HFM* and heater, or presence of a guard ring). Finally, other possible sources of measurement errors, such as air gaps between *HFM* and specimen because of poor installation issues were studied.

Also in these analyses, the EN ISO 13786 dynamic parameters were calculated and compared to those obtained from the calibrated model (Table 3).

Table 3: Impact of guard ring and HFM poor installation on dynamic thermal parameters.

	Y_{ie} [W m^{-2} K^{-1}]	Deviations from calibrated model	t_{ie} [h]	Deviations from calibrated model
Numerical model including guard ring	0.1400	-0.34 %	11.78	0.28 %
Numerical model with air gap between *HFM* and wood	0.1288	-8.27 %	12.01	2.27 %

3.4.1 Convective boundary conditions: Convective processes induced by forced convection through over the *HFM* surface may have essential influence on results obtained by the sensor readings (Pernigotto *et al.*, 2015). So far, all simulated heat fluxes refer to the contact area between *HFM* and timber wall. Varying the position though the *HFM*, it can be appreciated a different level of noisiness in the results. For example, in Figure 10, the heat fluxes simulated at the center of the *HFM* and at the surface exposed to the air gap are compared to those at

the interface with the specimen: the noisiness increases with the proximity to the air gap. In particular, the heat fluxes simulated at the *HFM* surface exposed to the air gap are affected by a noise similar to the one observed in the experimental ones. Indeed, because of the *HFM* installation on the planar surface of the specimen, there is a variation on the air gap thickness which can cause some turbulences and emphasize some unsteadiness in the behavior of the fan. According to Flanders (1985, 1994), this can cause an error to the *HFM* measurement which can be reduced, for example, by installing a tape through over the *HFM* and its edges (1985). The efficacy of this solution will be tested and improved both experimentally and numerically in further developments of the current setup, in order to optimize the measurement quality by minimizing the noise effects.

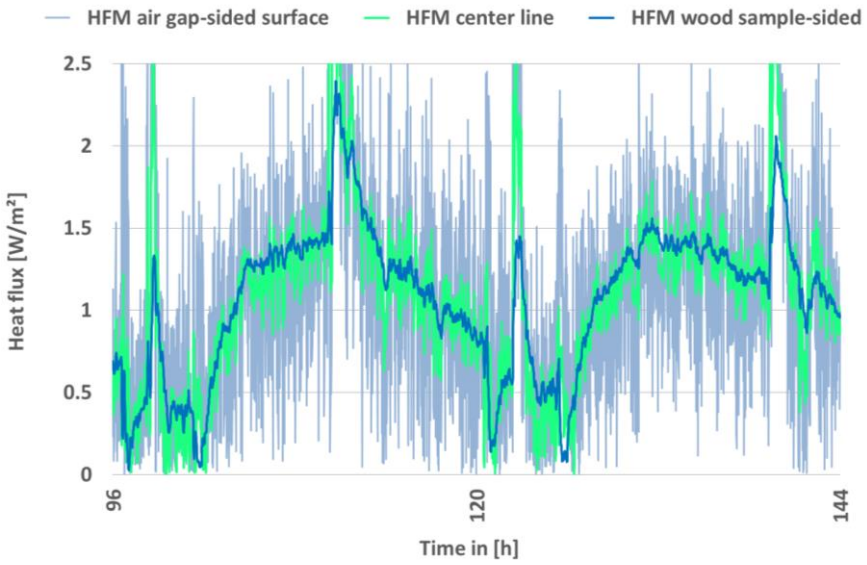

Figure 10: Different output positions for heat flux.

3.4.2 Conditions with potential impact on one-dimensional heat flux formation: The next analyses focus on the assumption of one-dimensional heat flux through the test specimen. In Figure 11**,** heat propagation within the timber wall is shown in temperature fields of different time steps. Due to different sizing of sample and electrical resistance, heat distribution across the sample is inhomogeneous (Figure 11a - 11c). Starting at time 103 h (Figure 11a), the external surface is excited by the electrical resistance. The influence of inhomogeneous temperature boundary conditions is clearly visible at this stage, and is even more emphasized after one hour (i.e., time 104 h in Figure 11b). After 10 hours, highest mean temperature is reached within the specimen (i.e., time 113 h in Figure 11c). By comparison, a variant with homogeneous temperature boundary condition results in a one-dimensional heat flux formation (Figure 11d). As it can be seen, the same size for specimen and electrical resistance would be of benefit but the impact of multi-dimensional heat flux on the *HFM* is negligible.

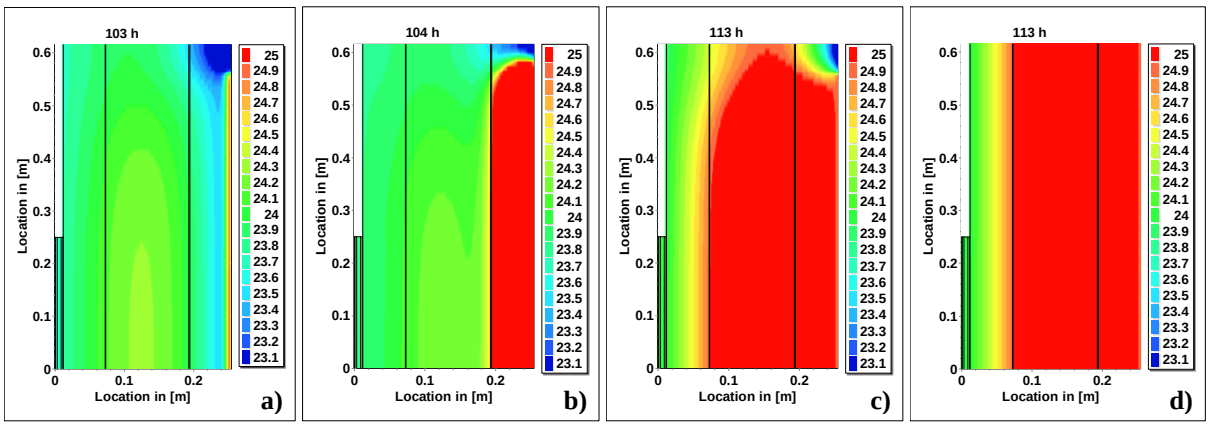

Figure 11: Temperature fields.

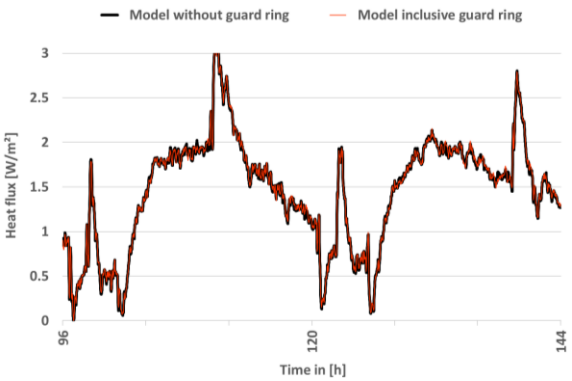

Figure 12: Influence of a guard ring around the *HFM* on numerical results.

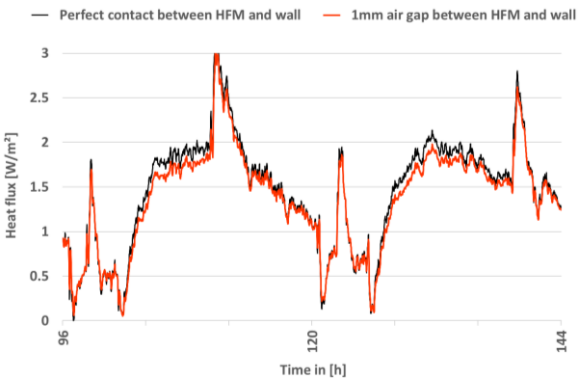

Figure 13: Influence of a contact resistance between *HFM* and specimen on numerical results.

For reaching one-dimensional heat flux conditions, a guard ring can be installed around the *HFM*. Within the numerical model, a guard ring with *HFM*-similar properties was simulated around the *HFM*, covering the surface area of our wooden test specimen completely. Differences within the simulated heat flux of initial and modified numerical models are marginal, as it can be seen in Figure 12.

3.4.3 Effects of *HFM* installation issues: If the *HFM* is not attached properly to a specimen's surface, the contact resistance can affect the measurement accuracy. For this reason, in the experimental setup a thin layer of heat conducting paste was used. However, considering the development of in-situ dynamic measurement approaches, imprecise *HFM* installations can more easily occur and, thus, the evaluation of their impact on the final results is worth of investigation. Consequently, the calibrated model was modified by adding a 1 mm thick air gap between the *HFM* and the specimen.
As showed in Figure 13, the main effect is a reduction of heat flux amplitudes and peaks. Periodic thermal transmittance changes substantially, showing a deviation of -8.27 % from the values of the calibrated numerical model while deviations in terms of time shift are much lower (2.27 %).

4. CONCLUSIONS

In this work, a hotbox apparatus equipped with heat flow meter at the Free University of Bozen-Bolzano was modified in order to allow dynamic tests aimed at calculating EN ISO 13786 dynamic parameters (i.e., periodic thermal transmittance, decrement factor and time shift). Exploiting the results of a test on a timber wall, a calibrated numerical model was used to assess the impact of different sources of measurement errors, in the perspective of further developments of methodologies for in-situ evaluations of the dynamic parameters through the data monitored by heat flow meters. In particular, we focused on the impact of different boundary conditions (e.g., convective conditions, contact resistances, homogeneity of heat flow).
We observed that the measurement of the heat flux by the heat flow meter is affected by some noisiness. Further developments will involve CFD analysis of alternative strategies to reduce the impact of turbulences and unsteady air flow conditions adjacent to the sensors first for the use in controlled environment and then in-situ. The impact of some setup elements which may affect the required one-dimensional heat flux, such as the size of the electrical heater inducing the periodic forcing solicitation and the presence of a guard ring around the heat flow meter, was investigated and found negligible. Finally, we assessed the extent to which some installation errors of the heat flow meter can affect the results of the test. Indeed, while heat conducting paste can be used in controlled environment, the same cannot be allowed for in-situ tests. The presence of small air gaps between the sensor and the wall were found relevant, especially concerning the assessment of the periodic thermal transmittance.
Thanks to the findings of this preliminary research, new modifications will be applied to the modified hotbox, which will be used to collect more data exploitable for the development of dynamic testing procedures also to assess the EN ISO 13786 dynamic parameters of the existing building stock.

REFERENCES

Brown, C. W., and D. G. Stephenson. 1993a. A guarded hot box procedure for determining the dynamic response of full-scale wall specimens - Part I. *ASHRAE Transactions*, 99(1): 632–642.

Brown, C. W., and D. G. Stephenson. 1993b. Guarded hot box measurements of the dynamic heat transmission characteristics of seven wall specimens - Part II. *ASHRAE Transactions*, 99(1): 643–660.

European Committee for Standardization (CEN). 1998. *EN 1934: Thermal performance of buildings - Determination of thermal resistance by hot box method using heat flow meter*. Brussels, Belgium.

European Committee for Standardization (CEN). 2007a. *EN ISO 13786: Thermal performance of building components - Dynamic thermal characteristics - Calculation methods*. CEN: Brussels, Belgium.

European Committee for Standardization (CEN) 2007b. *EN ISO 6946: Building components and building elements - Thermal resistance and thermal transmittance - Calculation method*. CEN: Brussels, Belgium.

European Directive 2010/31/EU of the European Parliament and of the Council of 19 May 2010 on the energy performance of buildings, *Official Journal of the European Union*.

Flanders, S. N. 1985. Heat flow sensors on walls- What can we learn? In E. Bales, M. Bomberg, and G. E. Courville (Eds.), *Building applications of heat flux transducers* (pp. 140–159): Philadelphia, U.S..

Flanders, S. N. 1994. Heat flux transducers measure in-situ building thermal performance. *Journal of Building Physics*, 18: 28–52.

Grunewald, J. 1997. *Diffuser und konvektiver Stoff- und Energietransport in kapillarporösen Baustoffen*. PhD Thesis. Dresden, Germany.

Italian Minister Decree 26/06/2015, *National Official Gazette* no. 162, July 15 2015.

Kollmann, F. 1982. *Technologie des Holzes und der Holzwerkstoffe: Band 1: Anatomie und Pathologie, Chemie, Physik, Elastizität und Festigkeit*. Berlin: Springer-Verlag.

Martín, K., I. Flores, C. Escudero, A. Apaolaza and J. M. Sala. 2010. Methodology for the calculation of response factors through experimental tests and validation with simulation. *Energy and Buildings*, 42(4): 461–467.

Martín, K., A. Campos-Celador, C. Escudero, I. Gómez and J. M. Sala. 2012. Analysis of a thermal bridge in a guarded hot box testing facility. *Energy and Buildings*, 50: 139–149.

Nicolai, A. 2008. *Modelling and Numerical Simulation of Salt Transport and Phase Transitions in Unsaturated Porous Building Materials*. PhD Thesis. Printed at Institute of Building Climatology - Dresden University of Technology: Dresden, Germany.

Nicolai, A. 2011. *Towards a Semi-Generic Simulation Framework for Mass and Energy Transport in Porous Materials*. Proceedings of the 9th Nordic Symposium on Building Physics (pp. 559–566).

Pernigotto, G., A. Prada, F. Patuzzi, M. Baratieri and A. Gasparella. 2015. Characterization of the dynamic thermal properties of the opaque elements through experimental and numerical tests. *Energy Procedia*, 78: 3234 – 3239.

Press, W. H., S. A. Teukolski, W. T. Vetterling and B. P. Flannery. 2007. *Numerical Recipes 3rd Edition: The art of scientific computing*. Cambridge University Press: Cambridge, U.K..

Sala, J. M., A. Urresti, K. Martín, I. Flores, and A. Apaolaza 2008. Static and dynamic thermal characterisation of a hollow brick wall: Tests and numerical analysis. *Energy and Buildings*, 40(8): 1513–1520.

Ulgen, K. 2002. Experimental and theoretical investigation of effects of wall's thermophysical properties on time lag and decrement factor. *Energy and Buildings*, 34(3): 273–278.